Mapping of Fabry-Perot and Whispering Gallery Modes in GaN microwires by Nonlinear imaging

Author(s):
Berdnikov, Yury; Shtrom, Igor; Rozhavskaya, Mariya; Lundin, W V; Hendricks, Nicholas; Grange, Rachel; Timofeeva, Maria

Publication date:
2021-10

Permanent link:
https://doi.org/10.3929/ethz-b-000495883

Originally published in:
Nanotechnology 32(40), https://doi.org/10.1088/1361-6528/ac1017

Funding acknowledgement:
150609 - Nonlinear Core-Shell Nanomaterials for Photonic Applications (SNF)
163916 - All-Dielectric and Hybrid Nanostructures for Biophotonic Applications (SNF)
179966 - All-dielectric nanowires as building blocks for nonlinear photonics (SNF)
714837 - Second-Order Nano-Oxides for Enhanced Nonlinear Photonics (EC)

Mapping of Fabry-Perot and Whispering Gallery Modes in GaN microwires by Nonlinear imaging

To cite this article before publication: Yury Berdnikov *et al* 2021 *Nanotechnology* in press https://doi.org/10.1088/1361-6528/ac1017

IOP Publishing Journal Title
Journal **XX** (XXXX) XXXXXX https://doi.org/XXXX/XXXX

Mapping of Fabry-Perot and Whispering Gallery Modes in GaN microwires by Nonlinear imaging

Yury Berdnikov,[1] Igor Shtrom,[1,2] Maria Rozhavskaya,[3], Wsevolod Lundin,[4] Nicholas Hendricks,[5] Rachel Grange,[5] and Maria Timofeeva [5]

[1] St. Petersburg University, Universitetskaya Emb. 13B, 199034, Saint-Petersburg, Russia
[2] Institute for Analytical Instrumentation RAS, 190103, Saint-Petersburg, Russia
[3] Soitec, Chemin des Franques, 38190, Bernin, France
[4] Ioffe Institute, Politekhnicheskaya 26, 194021, Saint-Petersburg, Russia
[5] ETH Zurich, Optical Nanomaterial Group, Institute for Quantum Electronics, Department of Physics, Auguste-Piccard Hof 1, 8093 Zurich, Switzerland

E-mail: mtimo@phys.ethz.ch

Received xxxxxx
Accepted for publication xxxxxx
Published xxxxxx

Abstract

Engineering nonlinear optical responses at the microscale is a key topic in photonics for achieving efficient frequency conversion and light manipulation. Gallium nitride (GaN) is a promising semiconductor material for integrated nonlinear photonic structures. In this work, we use epitaxially grown GaN microwires as nonlinear optical whispering gallery and Fabry-Perot resonators. We demonstrate an effective generation of second-harmonic and polarization-dependent signals of whispering gallery and Fabry-Perot modes under near-infrared excitation. We show how the rotation of the excitation polarization can be used to control and switch between Fabry-Perot and whispering gallery modes in tapered GaN microwire resonators. We demonstrate the enhancement of two-photon luminescence in the yellow-green spectral range due to efficient coupling between whispering gallery, Fabry-Perot modes, and excitonic states in GaN. This luminescence enhancement allows us to conveniently visualize whispering gallery modes excited with a near-infrared source. Such microwire resonators can be used as compact microlasers or sensing elements in photonic sensors.

Keywords: GaN, second harmonic generation, mode imaging

1. Introduction

Semiconductor III-V nano- and microwires (MWs) are considered as building blocks for photonic and optoelectronic devices. Small footprint and effective strain relaxation on the sidewalls provide high crystalline quality in MWs and open up the opportunity for integration of wide-bandgap semiconductors with silicon platform [1–3]. GaN is one of the most promising III-V semiconductor materials for applications in nonlinear photonics due to strong second and third order nonlinear optical properties, direct bandgap (3.4 eV) and compatibility with high operational temperatures (melting point is 2500 °C) [4,5]. The non-centrosymmetric crystal structure of GaN exhibits prominent piezo-electric properties suitable for applications in integrated electro-optical components and sensing devices [6,7].

Epitaxially grown GaN MWs typically have a wurtzite crystal structure, a hexagonal cross-section and smooth side facets. Hence, GaN MWs naturally suit potential applications as optical resonators [8,9] for integrated lasers [10,11] and sensors [6,12]. Previous studies have shown how GaN nanostructures can be used for confinement of whispering gallery (WGM) and Fabry-Perot (FPM) modes [13–16].

Optical resonators supporting WGM can be applied for cavity devices with exceptional properties such as small mode volume, high power density, and narrow spectral linewidth [12,17]. Moreover, such cavity modes can be coupled to strong exciton resonances when their frequencies are close to each other [18–20]. However, the key challenge in the development of WGM resonators is to design and fabricate the nanostructures that will efficiently confine WGMs.

The earlier studies of FPMs in GaN and GaAs MWs have demonstrated efficient second-harmonic generation (SHG) [21–24], which can be applied to frequency conversion devices, including ultraviolet (UV) and visible range lasers integrated with near-infrared (NIR) sources. The III-V MWs are promising components for integrated nanosystems since they can be used as elements of both active devices and passive interconnectors [25]. One of the main advantages of GaN MWs is that they can be synthesized in scalable epitaxial processes on different substrates, including silicon. However, control and characterization of the modes excited in MWs resonators remain challenging and require new advanced approaches.

Previous works demonstrated nanoscale imaging using electron energy loss spectroscopy or cathodoluminescence [26]. Despite the high resolution of luminescence mapping, these methods rely on sophisticated electron microscopy equipment and use the excitation by the electron beam rather than optical pumping and thus cannot be used to study optical nonlinear effects. Recording of the nonlinear response at the nanoscale over a broad range of wavelengths and polarizations of the incoming excitation laser beam may require sophisticated scanning methods which are time-consuming and need expensive components [27].

Far-field nonlinear optical microscopy is a fast non-invasive non-scanning technique that allows high-resolution mode imaging in nano- and microresonators [28,29]. Spatial information obtained from mode mapping is essential for the studies of local field distribution and enhancement [30,31] as well as diagnostics of devices in operation [32,33].

Our study shows how epitaxially grown GaN MWs can be employed as WGM resonators in the nonlinear optical regime. We demonstrate how the far-field nonlinear imaging is used for non-invasive investigation and visualization of WGM and FPM coupled with excitonic states in GaN MW resonators under NIR excitation. Within this approach we also demonstrate how polarization of the pump excitation can be used to switch the intensity of FPM and WGM inside MW resonator. The aim of this study is to obtain new means of all-optical control and switching of the confined modes, which is in high demand for various nanophotonic applications, such as integrated lasers, photonic sensors, and optical circuits.

2. Results and discussion

2.1 Microwires synthesis and morphology studies

The GaN MW resonators were grown by metal-organic chemical vapor deposition (MOCVD) on sapphire substrates catalyzed by Ti films. The details of the fabrication method are presented in our previous work [34], and in Supplementary Materials (Section 1). The MWs are formed along the c-axis and show extraordinary high elongation rate, which reduces GaN deposition times down to 20 min [34] in comparison to few hours in standard MOCVD growth. The synthesized GaN MWs are slightly tapered and have symmetric hexagonal cross-section and flat top facets. Figure 1 (a) and (b) shows side and top-view SEM images of GaN MWs and figure 1(c) shows a MW mechanically transferred on an ITO grid.

Nonlinear optical measurements are typically sensitive to facet roughness [35]. Hence, the smoothness of MW sidewalls was verified by atomic force microscopy (AFM). The details of the AFM characterization are given in Supplementary Materials (Section 2).

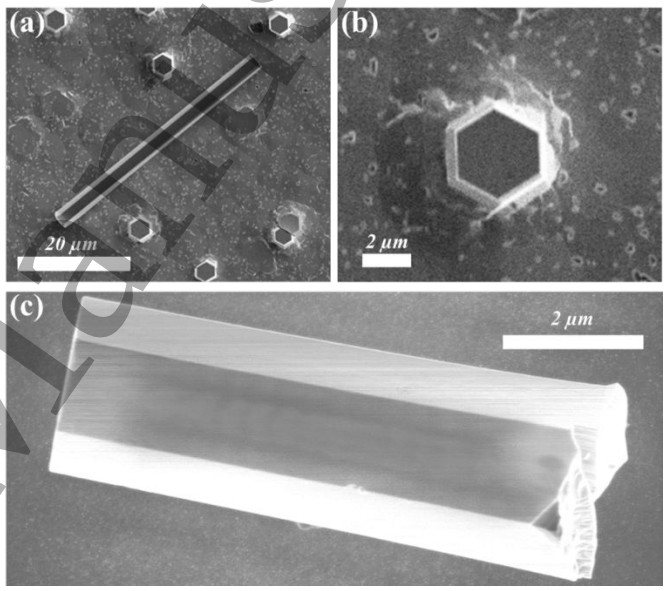

Figure 1. GaN MWs with hexagonal top facet on sapphire substrate (a) and (b). GaN MW after transfer to ITO grid for nonlinear optical characterization (c).2.2 Microwire optical characterization

A home-built non-scanning transmission nonlinear optical microscope [36,37] was used to characterize nonlinear optical performance of GaN MWs resonators. In the microscope the samples were excited with Ti: Sapphire pulsed (80 MHz) laser source that can operate in the region from 690 nm to 1000 nm. Additionally, the setup was equipped with a BBO crystal that allows to double the frequency of excitation from the NIR laser source to the UV range from 345 to 390 nm.

The samples of GaN MWs were transferred on the transparent ITO substrates and placed in the focal plane of the incident polarized laser beam. The setup allows one to vary the polarization of the incident beam from parallel to the long axis of the MW to perpendicular to it. In the output signal, we

acquired the spectra using the spectrometer and the spatial mode images with an electron-multiplying charge-coupled device (CCD) camera. Thus, we investigated linear and nonlinear optical responses of the synthesized MWs from UV and NIR excitation, respectively. In this study the linear optical response was obtained under UV excitation at 370 nm, which is close to the wavelength equivalent of the GaN bandgap [5].

The nonlinear response from GaN MWs was obtained under NIR excitation of 740 nm, about twice the wavelength of the bandgap. Thus, the recorded nonlinear response was stimulated by the absorption of two photons. After the sample, the NIR excitation wavelength was filtered out from the output signal. More technical details of sample preparation and optical measurements are given in Supplementary Materials (Section 1).

Figure 2 (a) and (b) shows the overlaid SEM and CCD images obtained under UV and NIR excitation, respectively. In both cases the fractured regions at the top and the bottom of the MW show more intense luminescence than the central parts of the MWs. Under UV excitation, the central parts of the MWs show the bright lines at the centers of three MW facets (figure 2(b)). Meanwhile, under the NIR excitation, the maxima of intensities are observed only at the specific diameters within the central parts of MWs (figure 2(a)). The signal in figure 2(a) presents the compact pointed three dots patterns that are visible in the centers of MW facets that we relate to the WGM confined in the MW resonator.

Figure 2 (c) shows typical examples of spectra of the tapered GaN MW acquired under UV (370 nm) and NIR (740 nm) excitation. The corresponding spectra in figure 2(c) demonstrate broad yellow-green luminescence (YGL). In previous studies, the YGL was attributed to defect states concentrated at the surface of GaN MW sidewalls [38,39]. Besides the YGL band, the spectrum under NIR excitation shows the peak around 370 nm, which combines the SHG at half of the incident field wavelength and the near band edge (NBE) emission.

The spectra and CCD images under NIR excitation are sensitive to the polarization of the incident laser beam, as shown in figure 3 (a, b). The mode imaging in figure 3(a) shows the shape variation of the luminescence patterns with the change of excitation polarization. The three-dot patterns have the maximum intensity when the incident light is polarized along the MW axis (angle $\theta = 0°$) and are not visible when polarization of the incident beam is 90° rotated.

The spectra in figure 3(b) were obtained after filtering most of the incident NIR light and normalized by the intensity of unfiltered incident field (740 nm). The peak near 370 nm corresponding to SHG and NBE signal shows only slight intensity variation with the change of excitation polarization. Meantime, the intensity of the YGL peak varies from almost zero to twice the intensity of the unfiltered incident field.

Figure 3(c) shows that the normalized intensities of the three-dot pattern in CCD images (blue circles labelled "CCD image") are well-correlated with the normalized intensities of YGL parts of spectra (red squares labelled "Spectrum") as functions of polarization of the incident field. The grey solid line in figure 3(c) shows the cosine-squared function which gives a good approximation for both dependencies. In contrast to NIR excitation, both spectra and CCD images show no dependence on the polarization under UV excitation at 360 – 370 nm, which is illustrated in figure S3 in Supplementary Materials (Section 3).

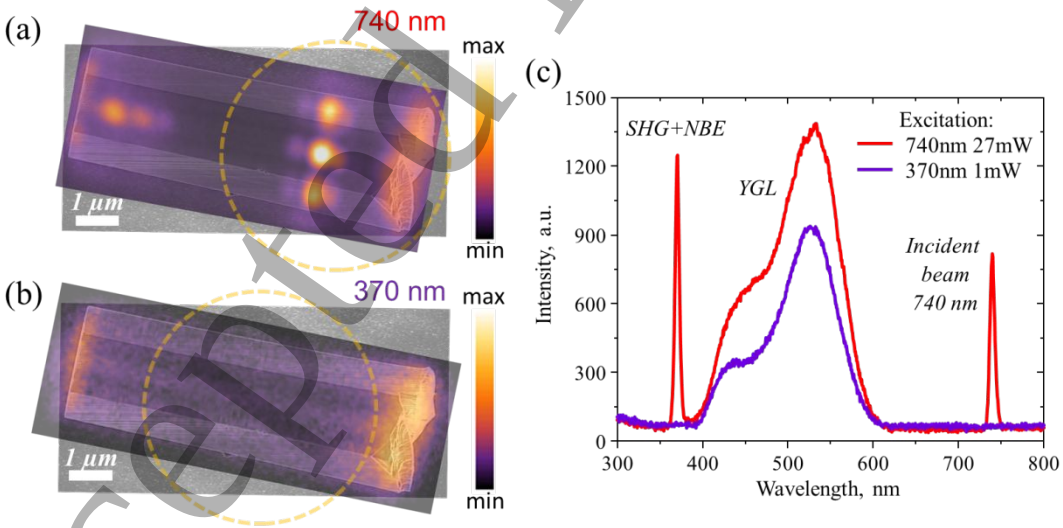

Figure 2. SEM image of GaN MW matched to CCD images acquired under NIR (a) and UV (b) excitation. The dotted circles show the approximated width of the laser beam. (c) photoluminescence spectra of GaN MW under UV excitation at 370 nm and NIR excitation at 740 nm.

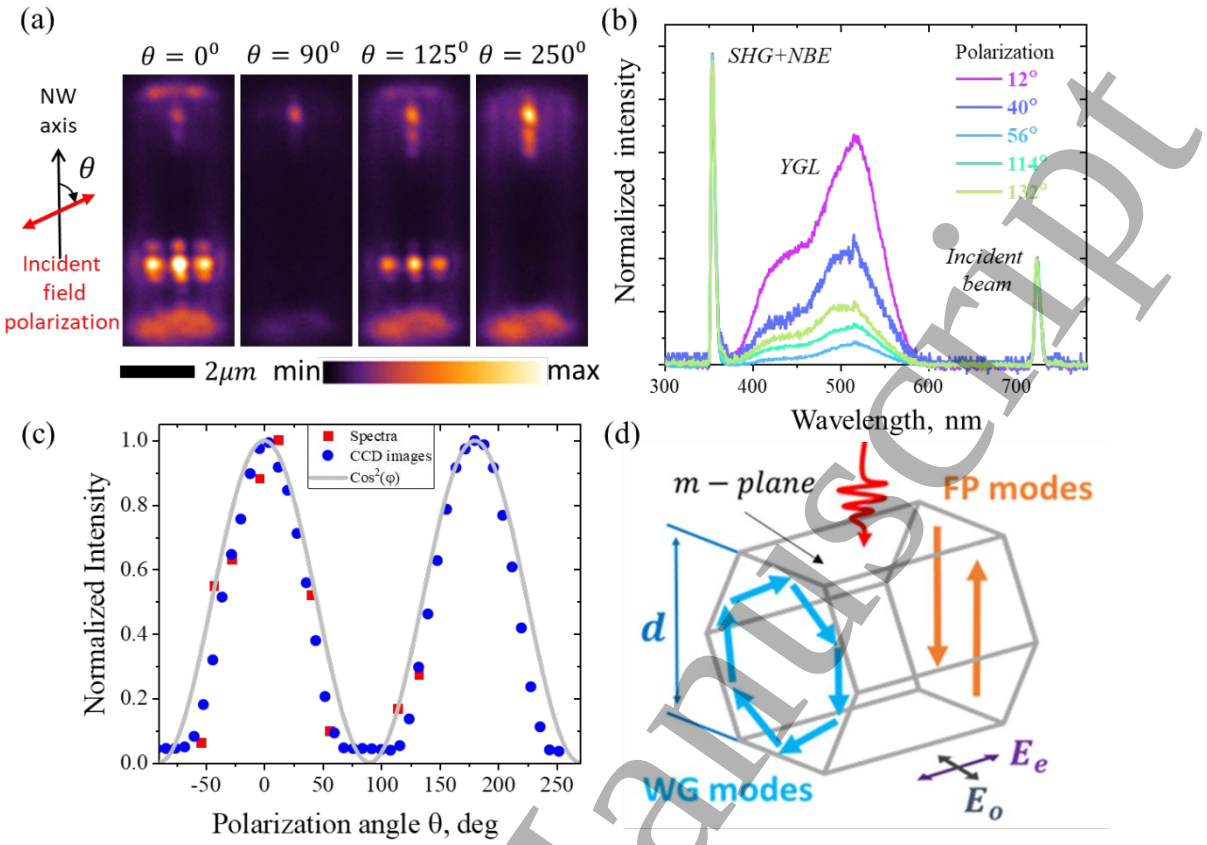

Figure 3. CCD images (a) and spectra (b) obtained under NIR excitation (740 nm). (c) Normalized intensities of YGL peaks in PL spectra (red squares labeled "Spectra"), the normalized intensity of three-dot pattern in the nonlinear CCD images (blue circles labelled "CCD image") at different angles of NIR (740 nm) excitation polarization. Error bars are comparable with the symbol size. (d) Schematic of WG and FP modes in wurtzite GaN MW resonator.

Next, we analysed the excited modes in GaN MW resonators to match the observed intensity patterns to the corresponding FPMs and WGMs. The confinement of FPMs and WGMs was earlier demonstrated in various GaN nanostructures with hexagonal cross-section: nanowires, nanorods, nanopyramids, etc. [13,14,17,40]. Figure 3(d) illustrates schematically the FPMs and WGMs in wurtzite GaN MW resonator. The size of the MW resonator is characterized by the distance between $\{10\bar{1}0\}$ facets (m-planes) denoted as d. In tapered MWs with d continuously changing along the wire axis, FPMs and WGMs contribute to the confinement of hybrid modes [41,42]. The modes of each of two types are characterized by the resonant facet separations d_{FP}^{m} and d_{WG}^{m} for m^{th} FPM and WGM, respectively. Within the plane-wave model the resonant diameters of GaN MWs can be calculated as [43]:

$$d_{FP}^{m} = m\,\lambda/2n \quad (1)$$

$$d_{WG}^{m} = \frac{\lambda}{3n}\left(m + \frac{6}{\pi}\left(\beta\sqrt{3n^2-4}\right)\right), \quad (2)$$

where λ is the wavelength, n is the refractive index and the parameter $\beta = n$ for TM polarization and $\beta = 1/n$ for TE polarization. We study wurtzite GaN MW growing along the c-axis associated to the extraordinary direction with $n = n_{ext}$ (TM). Thus, the ordinary direction with $n = n_{ord}$ (TE) is perpendicular to the MW axis as shown in figure 4(a).

The observed nonlinear YGL and UV luminescence under NIR excitation requires absorption of two or more photons simultaneously. Previous studies report considerable excitonic enhancement of two and three-photon absorption in GaN [44–46]. Therefore, the most effective FPM and WGM excitation is expected when coupled with excitonic state.

Previously, strong coupling between the exciton states and photonic cavity modes in GaN and ZnO was observed from cryogenic up to room temperatures [47–49]. From a quantum mechanical point of view the mixed state can be characterized by the superposition of excitonic and photonic wave functions [50]. Thus, the interaction between the cavity photons and excitons can be described in terms of exciton-polariton quasiparticles with energy E_p. Strong coupling in GaN microcavities results in splitting to two modes called upper

(UP) and lower polaritons (LP) with the energies about 3.40 eV and 3.35 eV, respectively [19]. Figure 4(a) shows the schematic diagram for transitions associated with polaritonic states [51].

Thus, we estimate the resonant facet separations for FPMs and WGMs (plotted in figure 4(c)) by inserting $\lambda = E_p/hc$ with E_p for UP or LP into eq. (1-2). Then we match the calculated facet separations with corresponding positions along the MW axis according to observed MW geometry. Circles in figure 4(d) show the measured facet separations d and their position along the MW axis extracted from SEM image. The polynomial fit was used to estimate the positions of FPMs and WGMs positions in the tapered GaN MW. These estimated mode positions match to the intensity maximums (dots patterning) in the CCD images in Fig 4(b). Thus, we can map the three-dot patterns to WGMs and single-dot maximums to FPMs.

Figure 4(b) shows that the observed features of the nonlinear response of GaN MWs are not specific for 740 nm excitation and were observed under the excitation with shorter and longer wavelengths. Figure 4(b) shows two clearly distinguishable three-dot patterns of WGMs coupled with excitonic states. More examples of spectra and CCD images for excitation at 770 nm are given in figure S4 in Supplementary Materials (Section 4).

The CCD images in figure 3(a) and figure 4(b) show only one or two WGMs which corresponds to the position of the exciting laser beam spot next to the wide end of the tapered MW. The other WGMs could also be visible when moving the position of the laser beam spot within the MW length, as illustrated in figure S5 (Supplementary Materials, Section 5).

The intensity patterns matched in our analysis to FPMs and WGMs depend differently on polarization of the incident light. Figure 3(a) shows three types of CCD images acquired at different excitation polarization: (i) when only FP mode is excited ($\theta = 90°$); (ii) when only WG mode is excited ($\theta = 0°$) or (iii) when both types of modes are excited ($\theta = 125°$). Thus, in the tapered GaN MWs studied in our work, the variation of polarization of NIR excitation allows selective excitation of FPM, WGM or both modes simultaneously. This approach gives the means for an all-optical switch of the resonance modes in hexagonal GaN resonators. Previously the selective excitation and switching between FP and WG modes were demonstrated by Baek et al. [52] where the selectivity was achieved by shifting the position of excitation from the center of the wire to its edge. Furthermore, the approach of [52] is limited to wires smaller than 1.5 μm in diameter and demonstrated only for UV excitation. Our approach uses NIR excitation and is suitable for large rods while the tapered shape allows switching without changing the position of excitation by varying the incoming polarization.

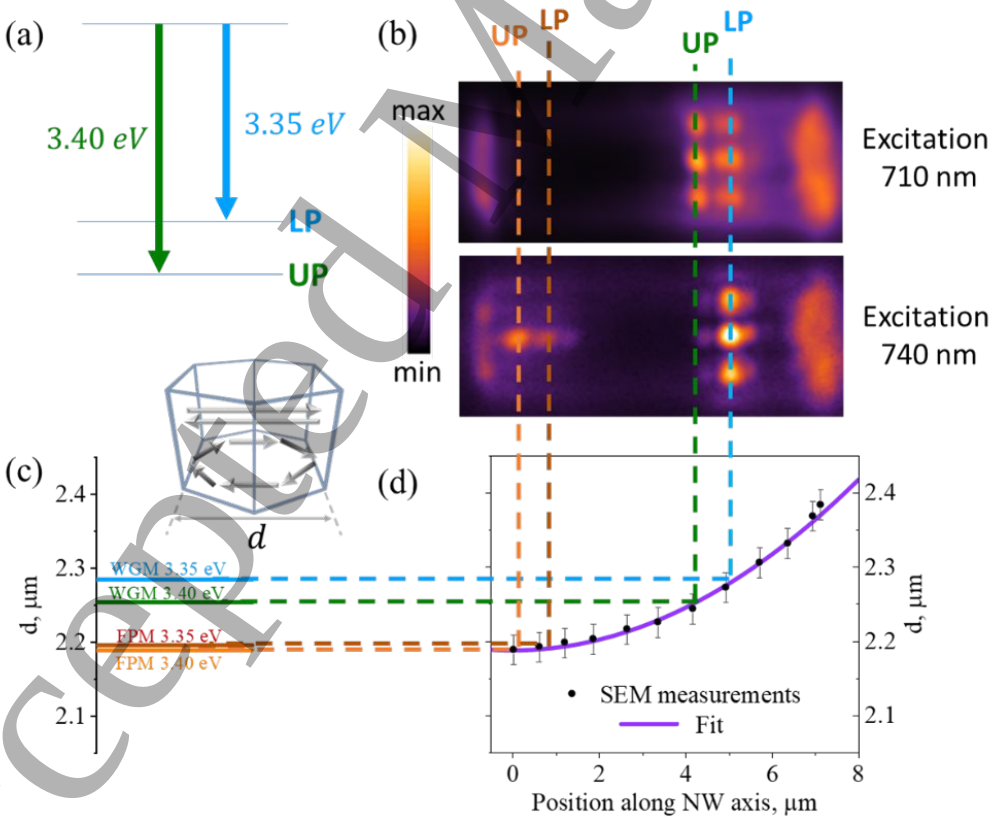

Figure 4. Schematic diagram for polaritonic transitions (a). Resonance facet separations (c) matched to the dotted patterns in CCD images (b) via the dependence of facet separation on position along the axis of the tapered MW(d).

We have found that the spectra of dotted patterns include the YGL band. As we show in Supplementary Materials (Section 6) the dotted patterns of luminescence maxima remained visible when the 400 nm long-pass filter was placed between the sample and the CCD camera. As we have shown in figure 4, the position of the three-dot pattern intensities corresponds to the WGM resonance diameter. Thus, we conclude that the coupling between excitonic states and WGMs excited under NIR irradiation results in local enhancement of the YGL at resonant diameters. In our interpretation we assume Purcell enhancement of the defect-related yellow-green luminescence. Each defect in GaN is introduced either by Ga-vacancies or C incorporation at the surface of the microwire sidewalls is considered as a compact light source. C-related defects in GaN nanostructures grown via a MOCVD process are known to originate from trimethylgallium precursor molecules [38]. Emission strength of these light sources is considered to be proportional to the photonic density of states induced by the cavity modes.

On one hand, the presence of YGL is widely considered as an undesirable factor related to defect states [1,53,54]. Except for some attempts of controlled use of artificially created defects [55,56], most studies of YGL aim at the quenching of defect luminosity [39,53]. On the other hand, in this work for the first time the YGL serves as a tool for visualization of WGMs coupled with excitonic states in the nanostructures, which cannot be observed directly. In hexagonal GaN MW cavities the WGM intensity has maximums in the directions along the MW facets [57], and minimums at the 90° angle to the m-plane facet (see figure 4(c)). In our setup we collect the signal in the latter direction, meanwhile, the YGL enhanced by WGM allows its visualization at the normal orientation to the sidewall plane.

3. Conclusions

In conclusion, we demonstrated that the Ti-assisted growth of GaN MWs by MOCVD provide the means for fast fabrication of optical FPM and WGM microresonators. We presented the approach to visualize WGMs and FPMs in tapered GaN MWs. Optical modes can be mapped and characterized via far-field nonlinear imaging and spectroscopy under UV and NIR excitation. We imaged WGMs and FPMs coupled with excitonic states excited with NIR sources. The obtained CCD images show that the patterns of nonlinear luminosity correspond to YGL enhanced at WG and FP resonant diameters. We demonstrated the selection between FPM and WGM confined in the tapered GaN MWs controlled by polarization of the incident laser beam. We believe that the suggested method of nonlinear optical characterization may be implemented for further studies of the light-matter interaction in semiconductor MWs. GaN MWs characterized in our work can be used as all-optical switching resonators supporting the high-quality WGM modes. Such MW resonators can be applied as a building blocks for compact frequency converting WGM microlasers, optical sensors and other light sources that can be controlled by the excitation polarization.

Acknowledgements

The authors thank A. V. Kavokin, M. Yu. Petrov and R.V. Cherbunin for fruitful discussions. Y. B. and I. S. acknowledge St. Petersburg State University for the research grant 75746688. The authors thank the Scientific Centre for Optical and Electron Microscopy (ScopeM) of ETH Zurich. This work was supported by the Swiss National Science Foundation grant 150609, 163916 and Ambizione grant no 179966, by the European Union's Horizon 2020 research and innovation program from the European Research Council under the Grant Agreement No 714837 (Chi2-nano-oxides).

References

[1] Barrigón E, Heurlin M, Bi Z, Monemar B and Samuelson L 2019 Synthesis and Applications of III–V Nanowires *Chem. Rev.* **119** 9170–220

[2] Quan L N, Kang J, Ning C-Z and Yang P 2019 Nanowires for Photonics *Chem. Rev.* **119** 9153–69

[3] Yuan X, Pan D, Zhou Y, Zhang X, Peng K, Zhao B, Deng M, He J, Tan H H and Jagadish C 2021 Selective area epitaxy of III–V nanostructure arrays and networks: Growth, applications, and future directions *Appl. Phys. Rev.* **8** 021302

[4] Stassen E, Pu M, Semenova E, Zavarin E, Lundin W and Yvind K 2019 High-confinement gallium nitride-on-sapphire waveguides for integrated nonlinear photonics *Opt. Lett.* **44** 1064

[5] Hassan A, Savaria Y and Sawan M 2018 GaN Integration Technology, an Ideal Candidate for High-Temperature Applications: A Review *IEEE Access* **6** 78790–802

[6] Peng Y, Lu J, Peng D, Ma W, Li F, Chen Q, Wang X, Sun J, Liu H and Pan C 2019 Dynamically Modulated GaN Whispering Gallery Lasing Mode for Strain Sensor *Adv. Funct. Mater.* **29** 1905051

[7] Avit G, Robin Y, Liao Y, Nan H, Pristovsek M and Amano H 2021 Strain-induced yellow to blue emission tailoring of axial InGaN/GaN quantum wells in GaN nanorods synthesized by nanoimprint lithography *Sci. Rep.* **11** 6754

[8] Tessarek C, Dieker C, Spiecker E and Christiansen S 2013 Growth of GaN Nanorods and Wires and Spectral Tuning of Whispering Gallery Modes in Tapered GaN Wires *Jpn. J. Appl. Phys.* **52** 08JE09

[9] Jiao Q, Chen Z, Feng Y, Li S, Jiang S, Li J, Chen Y, Yu T, Kang X, Shen B and Zhang G 2016 The effects of nanocavity and photonic crystal in InGaN/GaN nanorod LED arrays *Nanoscale Res. Lett.* **11** 0–7

[10] To C H, Fu W Y, Li K H, Cheung Y F and Choi H W 2020 GaN microdisk with direct coupled waveguide for unidirectional whispering-gallery mode emission *Opt. Lett.* **45** 791

[11] Eaton S W, Fu A, Wong A B, Ning C-Z and Yang P 2016 Semiconductor nanowire lasers *Nat. Rev. Mater.* **1** 16028

[12] Foreman M R, Swaim J D and Vollmer F 2015 Whispering gallery mode sensors *Adv. Opt. Photonics* **7** 168

[13] Tessarek C, Heilmann M and Christiansen S 2014

Whispering gallery modes in GaN microdisks, microrods and nanorods grown by MOVPE *Phys. status solidi* **11** 794–7

[14] Coulon P-M, Hugues M, Alloing B, Beraudo E, Leroux M and Zuniga-Perez J 2012 GaN microwires as optical microcavities: whispering gallery modes Vs Fabry-Perot modes *Opt. Express* **20** 18707

[15] Høiaas I M, Liudi Mulyo A, Vullum P E, Kim D-C, Ahtapodov L, Fimland B-O, Kishino K and Weman H 2019 GaN/AlGaN Nanocolumn Ultraviolet Light-Emitting Diode Using Double-Layer Graphene as Substrate and Transparent Electrode *Nano Lett.* **19** 1649–58

[16] Liang Y, Zhu H, Zheng H, Tang Z, Wang Y, Wei H, Hong R, Gui X and Shen Y 2021 Competition of whispering gallery lasing modes in microwire with hexagonal cavity *J. Phys. D. Appl. Phys.* **54** 055107

[17] Yang S, Wang Y and Sun H D 2015 Advances and Prospects for Whispering Gallery Mode Microcavities *Adv. Opt. Mater.* **3** 1136–62

[18] Liew T C H, Glazov M M, Kavokin K V., Shelykh I A, Kaliteevski M A and Kavokin A V. 2013 Proposal for a Bosonic Cascade Laser *Phys. Rev. Lett.* **110** 047402

[19] Heo J, Jahangir S, Xiao B and Bhattacharya P 2013 Room-temperature polariton lasing from GaN nanowire array clad by dielectric microcavity *Nano Lett.* **13** 2376–80

[20] Das A, Heo J, Jankowski M, Guo W, Zhang L, Deng H and Bhattacharya P 2011 Room temperature ultralow threshold GaN nanowire polariton laser *Phys. Rev. Lett.* **107** 1–5

[21] Timofeeva M, Bouravleuv A, Cirlin G, Shtrom I, Soshnikov I, Reig Escalé M, Sergeyev A and Grange R 2016 Polar Second-Harmonic Imaging to Resolve Pure and Mixed Crystal Phases along GaAs Nanowires *Nano Lett.* **16** 6290–7

[22] Long J P, Simpkins B S, Rowenhorst D J and Pehrsson P E 2007 Far-field imaging of optical second-harmonic generation in single GaN nanowires *Nano Lett.* **7** 831–6

[23] Yu Y, Wang J, Wei Y-M, Zhou Z-K, Ni H-Q, Niu Z-C, Wang X-H and Yu S-Y 2017 Precise characterization of self-catalyzed III–V nanowire heterostructures via optical second harmonic generation *Nanotechnology* **28** 395701

[24] Carletti L, de Ceglia D, Vincenti M A and De Angelis C 2019 Self-tuning of second-harmonic generation in GaAs nanowires enabled by nonlinear absorption *Opt. Express* **27** 32480

[25] Kim S K, Kempa T J, Lieber C M and Park H G 2018 Nanowire Photonics and Their Applications *Computational Nanophotonics: Modeling and Applications* ed S Musa (CRC Press) pp 65–102

[26] Kennedy O W, White E R, Howkins A, Williams C K, Boyd I W, Warburton P A and Shaffer M S P 2019 Mapping the Origins of Luminescence in ZnO Nanowires by STEM-CL *J. Phys. Chem. Lett.* **10** 386–92

[27] Fetisova M, Kryzhanovskaya N, Reduto I, Zhurikhina V, Morozova O, Raskhodchikov A, Roussey M, Pélisset S, Kulagina M, Guseva Y, Lipovskii A, Maximov M and Zhukov A 2020 Strip-loaded horizontal slot waveguide for routing microdisk laser emission *J. Opt. Soc. Am. B* **37** 1878

[28] Grange R, Brönstrup G, Kiometzis M, Sergeyev A, Richter J, Leiterer C, Fritzsche W, Gutsche C, Lysov A, Prost W, Tegude F, Pertsch T, Tünnermann A and Christiansen S 2012 Far-Field Imaging for Direct Visualization of Light Interferences in GaAs Nanowires *Nano Lett.* **12** 5412–7

[29] Escalé M R, Sergeyev A, Geiss R and Grange R 2017 Nonlinear mode switching in lithium niobate nanowaveguides to control light directionality *Opt. Express* **25** 3013

[30] Zagonel L F, Mazzucco S, Tencé M, March K, Bernard R, Laslier B, Jacopin G, Tchernycheva M, Rigutti L, Julien F H, Songmuang R and Kociak M 2011 Nanometer Scale Spectral Imaging of Quantum Emitters in Nanowires and Its Correlation to Their Atomically Resolved Structure *Nano Lett.* **11** 568–73

[31] Usui S, Kitade S, Morichika I, Kohmura K, Kusa F and Ashihara S 2017 Near-Field Imaging of Infrared Nanoantenna Modes Under Oblique Illumination *J. Phys. Chem. C* **121** 26000–6

[32] Mujumdar S, Koenderink A F, Sünner T, Buchler B C, Kamp M, Forchel A and Sandoghdar V 2007 Near-field imaging and frequency tuning of a high-Q photonic crystal membrane microcavity *Opt. Express* **15** 17214

[33] McGehee W R, Michels T, Aksyuk V and McClelland J J 2017 Two-dimensional imaging and modification of nanophotonic resonator modes using a focused ion beam *Optica* **4** 1444

[34] Rozhavskaya M M, Lundin W V., Lundina E Y, Davydov V Y, Troshkov S I, Vasilyev A A, Brunkov P N, Baklanov A V., Tsatsulnikov A F and Dubrovskii V G 2015 Gallium nitride nanowires and microwires with exceptional length grown by metal organic chemical vapor deposition via titanium film *J. Appl. Phys.* **117** 024301

[35] Sivakov V A, Voigt F, Berger A, Bauer G and Christiansen S H 2010 Roughness of silicon nanowire sidewalls and room temperature photoluminescence *Phys. Rev. B* **82** 125446

[36] Timofeeva M, Lang L, Timpu F, Renaut C, Bouravleuv A, Shtrom I, Cirlin G and Grange R 2018 Anapoles in Free-Standing III–V Nanodisks Enhancing Second-Harmonic Generation *Nano Lett.* **18** 3695–702

[37] Saerens G, Lang L, Renaut C, Timpu F, Vogler-Neuling V, Durand C, Tchernycheva M, Shtrom I, Bouravleuv A, Grange R and Timofeeva M 2019 Image-based autofocusing system for nonlinear optical microscopy with broad spectral tuning *Opt. Express* **27** 19915

[38] Huang P, Zong H, Shi J, Zhang M, Jiang X, Zhong H, Ding Y, He Y, Lu J and Hu X 2015 Origin of 3.45 eV Emission Line and Yellow Luminescence Band in GaN Nanowires: Surface Microwire and Defect *ACS Nano* **9** 9276–83

[39] Li Q and Wang G T 2010 Spatial Distribution of Defect Luminescence in GaN Nanowires *Nano Lett.* **10** 1554–8

[40] Butler S, Jiang H, Lin J and Neogi A 2017 Hyperspectral Nonlinear Optical Light Generation from a Monolithic GaN Microcavity *Adv. Opt. Mater.* **5**

[41] Kirschbrown J R, House R L, Mehl B P, Parker J K and Papanikolas J M 2013 Hybrid standing wave and whispering gallery modes in needle-shaped ZnO rods: Simulation of emission microscopy images using finite difference frequency domain methods with a focused Gaussian source *J. Phys. Chem. C* **117** 10653–60

[42] Coulon P-M, Pugh J R, Athanasiou M, Kusch G, Le Boulbar E D, Sarua A, Smith R, Martin R W, Wang T, Cryan M, Allsopp D W E and Shields P A 2017 Optical properties and resonant cavity modes in axial InGaN/GaN nanotube microcavities *Opt. Express* **25** 28246–57

[43] Nobis T, Kaidashev E M, Rahm A, Lorenz M and

Grundmann M 2004 Whispering Gallery Modes in Nanosized Dielectric Resonators with Hexagonal Cross Section *Phys. Rev. Lett.* **93** 103903

[44] Lin K-H, Chern G-W, Huang Y-C, Keller S, DenBaars S P and Sun C-K 2003 Observation of huge nonlinear absorption enhancement near exciton resonance in GaN *Appl. Phys. Lett.* **83** 3087–9

[45] Yang H, Xu S J, Li Q and Zhang J 2006 Resonantly enhanced femtosecond second-harmonic generation and nonlinear luminescence in GaN film grown on sapphire *Appl. Phys. Lett.* **88** 161113

[46] Martins R J, Siqueira J P, Manglano Clavero I, Margenfeld C, Fündling S, Vogt A, Waag A, Voss T and Mendonca C R 2018 Carrier dynamics and optical nonlinearities in a GaN epitaxial thin film under three-photon absorption *J. Appl. Phys.* **123** 243101

[47] Trichet A, Médard F, Zúñiga-Pérez J, Alloing B and Richard M 2012 From strong to weak coupling regime in a single GaN microwire up to room temperature *New J. Phys.* **14** 073004

[48] Ghosh P, Yu D, Hu T, Liang J, Chen Z, Yingkai L and Huang M 2019 Strong exciton–photon coupling and polariton lasing in GaN microrod *J. Mater. Sci.* **54** 8472–81

[49] Jiang M, Tang K, Wan P, Xu T, Xu H and Kan C 2021 A single microwire near-infrared exciton–polariton light-emitting diode *Nanoscale* **13** 1663–72

[50] Timofeev V and Sanvitto D 2012 *Exciton Polaritons in Microcavities* vol 172 (Berlin, Heidelberg: Springer Berlin Heidelberg)

[51] Feltin E, Christmann G, Butté R, Carlin J-F, Mosca M and Grandjean N 2006 Room temperature polariton luminescence from a GaN/AlGaN quantum well microcavity *Appl. Phys. Lett.* **89** 071107

[52] Baek H, Hyun J K, Chung K, Oh H and Yi G-C 2014 Selective excitation of Fabry-Perot or whispering-gallery mode-type lasing in GaN microrods *Appl. Phys. Lett.* **105** 201108

[53] Demchenko D O, Diallo I C and Reshchikov M A 2013 Yellow luminescence of gallium nitride generated by carbon defect complexes *Phys. Rev. Lett.* **110** 1–5

[54] Liudi Mulyo A, Rajpalke M K, Kuroe H, Vullum P E, Weman H, Fimland B O and Kishino K 2019 Vertical GaN nanocolumns grown on graphene intermediated with a thin AlN buffer layer *Nanotechnology* **30**

[55] Berhane A M, Jeong K Y, Bodrog Z, Fiedler S, Schröder T, Triviño N V, Palacios T, Gali A, Toth M, Englund D and Aharonovich I 2017 Bright Room-Temperature Single-Photon Emission from Defects in Gallium Nitride *Adv. Mater.* **29**

[56] Saleem U, Birowosuto M D, Hou S, Maurice A, Kang T B, Teo E H T, Tchernycheva M, Gogneau N and Wang H 2018 Light emission from localised point defects induced in GaN crystal by a femtosecond-pulsed laser *Opt. Mater. Express* **8** 2703

[57] Dai J, XU C X, Zheng K, Ly C G and Cui Y P 2009 Whispering gallery-mode lasing in ZnO microrods at room temperature *Appl. Phys. Lett.* **95** 241110